Jurnal Ilmu Fisika
Vol. 17, No. 1, March 2025, pp. 78–87
ISSN: 1979-4657 (Print); 2614-7386 (Online)
https://doi.org/10.25077/jif.17.1.78-87.2025

Jurnal Ilmu Fisika
Open Access

Ionospheric Irregularities Related to Scintillation During Geomagnetic Storm in March, April, 2023 Over Indonesia

Angelikus Olla[1], Fernince Ina Pote[1], Asnawi Husin[2]

[1] Department of Physics, San Pedro Universty, Kupang, 85112, Indonesia
[2] Space Research Center, BRIN, Bandung, 40135, Indonesia

Article Info

Article History:

Received November 08, 2024
Revised February 07, 2025
Accepted February 09, 2025
Published online March 04, 2025

Keywords:

ionosphere
geomagnetic storm
scintillation
TEC
ROTI

Corresponding Author:

Angelikus Olla,
Email: angelikusolla@gmail.com

ABSTRACT

This study aims to analyze ionospheric irregularities in plasma structures on scales above 400 meters–several kilometers associated with scintillation using GPS satellite signal observation techniques. This study was conducted in the Indonesian region during the main phase of a strong category geomagnetic storm on March 23-24 and April 23-24, 2023 using Total Electron Content (TEC) and Rate of TEC Index (ROTI), from GPS receiver observations in Manado (1.34˚N-124.82˚E; -7.91˚S), Kupang (10.16˚S-123.67˚E; -19.38˚S), Bandung (6.9˚S-107.6˚E; 17.5˚S) and Biak (1.0˚S-136.0˚E; 12.18˚S). The results showed that during the geomagnetic storm on March 23-24, plasma irregularities, characterized by irregularities on a scale of more than 400 meters and evidenced by an increase in ROTI, were largely suppressed at all observation sites except Bandung. Likewise, most stations did not show a substantial increase in ROTI values in the subsequent storm on April 23-24, 2023, indicating continued suppression except for the Manado station. Furthermore, changes in TEC variations in response to the March 23-24 storm indicate that stations in Biak and Manado experienced positive storms (increase in TEC), while stations Bandung and Kupang experienced negative storms (decrease in TEC). In contrast, during the storm on April 23–24, 2023, all locations reported positive storms.

1. INTRODUCTION

The ionosphere is a part of the atmosphere at an altitude of 50-1000km from the earth's surface that contains ions and electrons useful for radio wave propagation. Ions and electrons in the ionosphere often experience disturbances, such as increases or decreases in the form of plasma bubbles. Space phenomena such as solar flares, coronal mass ejections, and geomagnetic storms are sources of ionospheric density disturbances.

The ionospheric irregularities in the plasma structure of the F layer on a scale of 310 to 400 meters, known as the first Fresnel zone of L frequency band radio waves (1-2 GHz), can be investigated using a Global Positioning System (GPS) receiver or Global Navigation Satellite System (GNSS) observation. The ionospheric irregularities on this scale can be measured from the strength (amplitude) of the GNSS signal, which is referred to as the scintillation index (S4) (Aol et al., 2020). Meanwhile, disturbance scales of 400 m to several km can be identified by calculating the Rate of TEC index (ROTI) (Vankadara et al., 2022). The occurrence of ionospheric irregularities causes fluctuations in the amplitude and phase of satellite signal radio waves in the L band known as Scintillation. Scintillation

usually occurs after sunset due to a decrease in electron density, also known as a plasma bubble. Signals or radio waves from satellites that pass through the scintillation area will experience fluctuations which can cause failure in satellite-based communication and navigation technology (Zhao et al., 2021).

The scintillation phenomenon which indicates the occurrence of plasma bubbles can be recognized from S4 data and ROTI data. However, the difference in the scale of this disturbance means that the scintillation from the ROTI data is not always followed by that from the S4 data. The relationship between S4 and ROTI has been reported to be not very strong, namely 0.5 to 0.6 (Abe et al., 2023).

Ionospheric irregularities occurrence rate was reported higher in the equinox months that is equinox March (March, April) and equinox September (September, October) depending on solar activity. It also declared that the occurrence rate of ionospheric irregularities experienced an asymmetry between the two equinoxes (Nguyen Thanh et al., 2021).

The ionosphere also experiences disturbances due to geomagnetic storms. Geomagnetic storms are classified based on the Dst index, including weak geomagnetic storms ($-50 < Dst \leq -30$ nT), moderate geomagnetic storms ($-100 < Dst \leq -50$ nT), strong geomagnetic storms ($Dst < 250 \leq Dst \leq 100$ nT), and severe geomagnetic storms (< -250nT) (Collado-Villaverde et al., 2024). Previous studies in different regions showed that ionospheric irregularities related to scintillation can be enhanced or inhibited during geomagnetic storms (Chen et al., 2023; Kassa et al., 2024; Olabode & Ariyibi, 2020; Ondede et al., 2022). The geomagnetic storm also fluctuated the TEC variation (Uga et al., 2024).

Although studies have been done regarding the effects of geomagnetic storms on ionospheric irregularities, investigations into the influence of geomagnetic storms, especially strong-category geomagnetic storms, on ionospheric irregularities associated with scintillation are still needed. Moreover, the variations in electron content during strong geomagnetic storms still need to be explained. Therefore, we are conducting a study that focuses on analyzing the occurrence of ionospheric irregularities associated with scintillation and electron content variation in the Indonesia region during strong category geomagnetic storms in March and April 2023. This study is needed because Indonesia is located at a low latitude magnetic region that allows for a high occurrence of ionospheric irregularities that have an impact on the propagation of radio waves. The results of this study are expected to give valuable information about the ionospheric irregularities with scale sizes 400m-several kilometers related to scintillation occurrence and the TEC variation over Indonesia during the strong geomagnetic storms.

We employed ROTI and TEC data from four GPS receivers in the Indonesia region to investigate the ionospheric irregularities and electron variation during strong geomagnetic storms. The TEC and ROTI were obtained from GPS receiver observations at Manado (Northern part of Indonesia), Kupang (Southern part of Indonesia), Bandung (Western part of Indonesia), and Biak (Eastern part of Indonesia) stations. The ROTI is used to observe the ionospheric irregularities in plasma structures on scales above 400 meters–several kilometers associated with scintillation. TEC is used to observe the variation in electron content.

2. METHOD

We used data obtained from four GNSS station sites based on data availability for ionospheric irregularities analysis. Unfortunately, other stations cannot be used due to concurrent data availability. However, spatially, these four stations are enough. Table 1 presents the geographic and geomagnetic coordinates of the available stations. Table 1 presents the geographic and geomagnetic coordinates of the available stations.

The World Data Center (WDC) for Geomagnetism Kyoto reports that throughout 2023 there were several strong geomagnetic storms where the Dst index value fell below -100nT. The geomagnetic storms occurred on March 23-24 2023 and April 23-24, 2023. The Dst index for March 23-24 and April 23-24,2023, is used to analyze the magnitude of the geomagnetic storm. ROTI parameter obtained from the GPS receiver's signal processing at four stations is used to investigate the impact of geomagnetic storms on ionospheric plasma density disturbances with scales above 400m-several kilometers associated with scintillation.

Table 1 Geographic and geomagnetic latitude of GPS/GNSS receiver station points.

Station	Geographic Latitude	Geographic Longitude	Magnetic Latitude
Bandung	6,9˚LS	107,6˚ BT	17.5˚S
Kupang	10.16˚LS	123,67˚BT	19,38˚S
Manado	1.34˚LU	124,82˚BT	7.91˚S
Biak	1,0˚ LS	136,0˚BT	12,18˚S

Furthermore, TEC obtained from the four GPS receivers, is used for total electron content variations analysis during geomagnetic storms. Table 1 shows the geographic and magnetic locations of the GPS receiver stations used in this study and the distribution of observation points shown in the map in Figure 1.

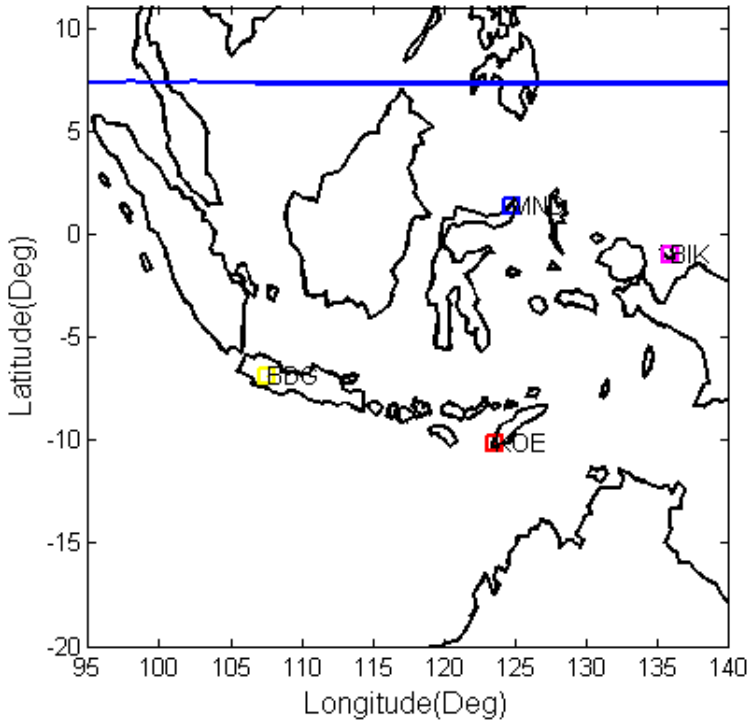

Figure 1 Locations of GPS receivers are marked with blue, red, yellow, and purple squares. The x and y axes show geographic coordinates (longitude, latitude) while the blue line shows the magnetic equator.

2.1 Total Electron Content (TEC)

The GPS/GNSS receiver is an instrument that records dual frequency satellite signals L1 (1.575 GHz) and L2 (1.22 GHz). One of the data from GNSS receiver observations is TEC which contains information about the amount of electron content in the ionosphere. TEC is obtained from several GNSS satellite signals orbiting in one day. TEC values from GPS receivers still contain biases (multipath effect) therefore data reduction with elevations below 30˚ is required. The TEC recorded by the GPS receiver is a slant TEC combination of phase (L) and pseudorange (P) signal measurement methods. Slant TEC can be calculated using equation (1).

$$STEC = \frac{1}{40.3} \times \left(\frac{1}{L1^2} - \frac{1}{L2^2}\right) \times (P_1 - P_2) \quad (1)$$

STEC: slant TEC (TECu), P1, P2: Pseudorange on L1 and L2, L1 and L2: signal frequency 1.2 (Hz). STEC can be expressed in vertical TEC (VTEC) using a thin-layer model approach.

$$VTEC = STEC \times cos\left[arc\sin\left(\frac{R_e cos\theta}{R_e + h_{max}}\right)\right] \quad (2)$$

Re: Distance from satellite to receiver (km), $hmax$: Maximum height of the ionosphere (350 km), θ: Elevation angle between receiver and satellite (°).

After getting the VTEC value, all of the average VTEC visible satellites for one minute of observation were then drawn to obtain 24 data, which represents 24 hours of observation (one day of observation). Furthermore, the daily observation data is tabulated in one month and plotted in a daily VTEC graph in one month to analyze the impact of geomagnetic storms on TEC variation.

2.2 Rate of TEC Index (ROTI)

The rate of TEC index (ROTI) is the standard deviation of TEC changes within 30 seconds called rate of change TEC (ROT). The ROT is used to calculate ROTI at 5-minute time intervals. The ROTI is used by researchers to investigate ionospheric irregularities such as plasma bubbles and scintillation based on Global Navigation Satellite System (GNSS) receiver observation (Li et al., 2022; Nguyen et al., 2022).

$$ROT = \frac{\Delta TEC}{\Delta t} = \frac{VTEC_k^i - VTEC_{k-1}^i}{(t_k - t_{k-1})} \quad (3)$$

i: the GPS receiver, t_k *:* time period (second). ROT is expressed in TEC units per minute (TECU/minute), 1TECU is equal to 10^{16} electrons/m^2.

$$ROTI = \sqrt{\langle ROT^2 \rangle - \langle ROT \rangle^2} \quad (4)$$

Ionospheric irregularities are classified as follows: no irregularity is seen when ROTI is less than 0.25 TECU/min, weak irregularity occurs when ROTI is between 0.25 and 0,5 TECU/min, moderate irregularity is observed when ROTI 0.5 and 1 TECU/min and strong irregularity when ROTI greater than 1 TECU/min (Kassa, 2024). We applied ROTI threshold 0,2 TECU/min in this study to detect the irregularities related to scintillation, and if the ROTI is less than the threshold, then the irregularities do not occur. The ROTI index that is obtained using equation (2) is tabulated and plotted into a ROTI graph every hour for one month to see the ionospheric irregularities related to scintillation events.

3. RESULTS AND DISCUSSION

3.1 Ionospheric Irregularities Related to Scintillation During Geomagnetic Storms March 23-24

TEC, ROTI, and Dst indices showing the occurrence of geomagnetic storms on 23-24 March 2023 are presented in a one-month observation graph, starting from Manado (North), Kupang (South), Bandung (West), and Biak (East) stations shown in Figures 2, 3, 4, and 5. The strong geomagnetic storm on March 23, 2023, started (initial phase) at 23.00 UT or 06.00 local time, and the Dst index fell to -102 nT. The Dst index continues to decrease significantly to -163 nT (main phase) on March 24, 2023, at 03.00 UT or 10.00 local time, after that the geomagnetic storm experiences a gradual recovery (recovery phase).

The ROTI parameters at Manado, Kupang, and Biak stations showed the inhibition of ionospheric irregularities associated with scintillation (ROTI value was <0.2 TECU/minute) on March 24, 2023, even though the geomagnetic storm was in the main phase. On the other hand, moderate ionospheric irregularities related to scintillation were observed at Bandung station during the geomagnetic storm, where the ROTI value was around 0.5≤ROTI≤1 TECU/minute.

If we compare the ROTI during the geomagnetic storm on March 23-24, 2023, at each station with the ROTI in the days before and after the geomagnetic, we found that the ionospheric irregularities due to scintillation occur more frequently when the geomagnetic are in quiet conditions than during the disturbed period. That is the characteristic of the scintillation occurrence in equinox months, with solar activity in 2023 reaching maximum. The trait of scintillation in March and April is characterized by an intense occurrence compared to the previous month, which is reported as the equinox season (Asnawi et al., 2021; Mondal et al., 2024).

TEC fluctuations in response to the geomagnetic storm on March 23-24, 2023, are showing different at each station. There was an increase in TEC (positive storm) at Manado and Biak on March 24, 2023, when the geomagnetic storm was in the main phase. In contrast, there was a decrease in TEC (negative storm) at Kupang and Bandung.

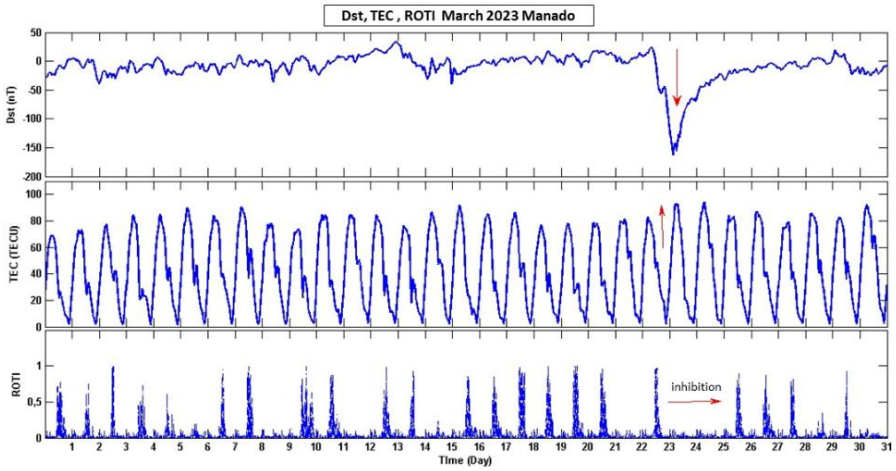

Figure 2 Dst, TEC, and ROTI indices for March at Manado.

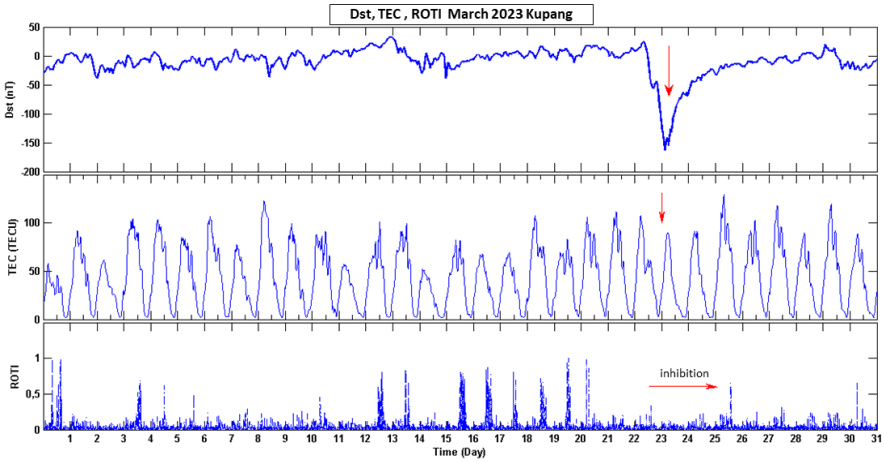

Figure 3 Dst, TEC, and ROTI indices for March at Kupang.

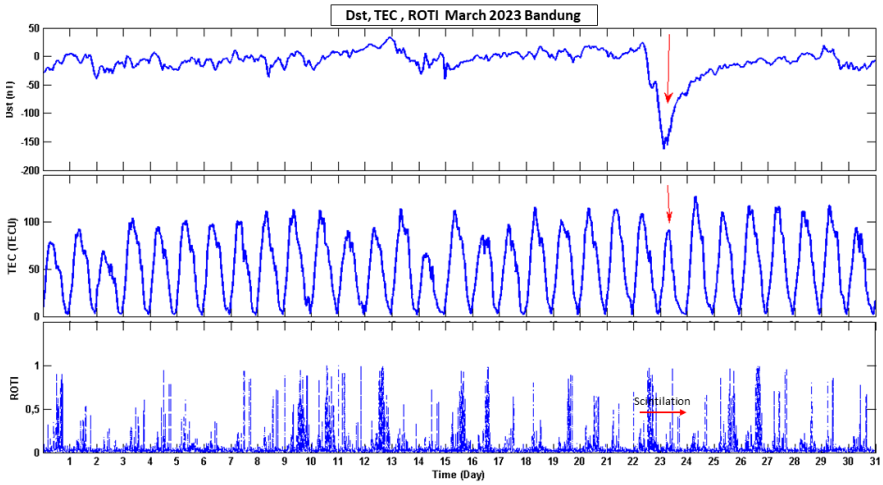

Figure 4 Dst, TEC, and ROTI indices for March at Bandung.

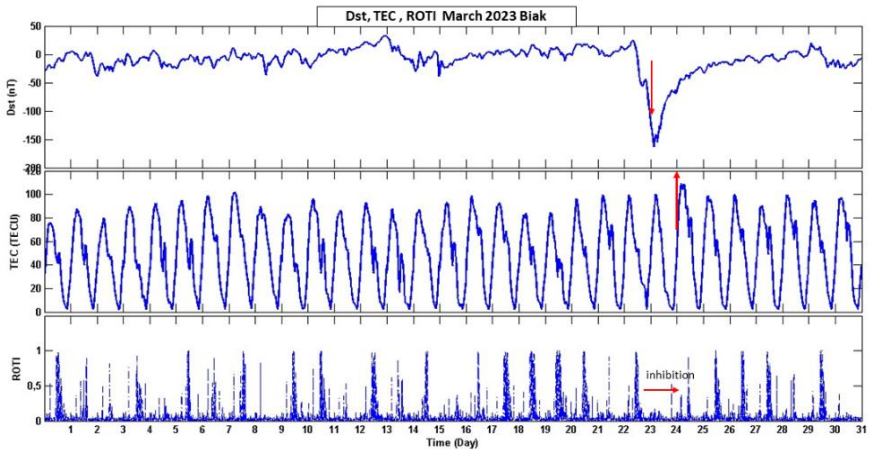

Figure 5 Dst, TEC, and ROTI indices for March at Biak.

3.2 Ionospheric Irregularities Related to Scintillation During Geomagnetic Storms April 23-24

Ionospheric irregularities related to scintillation and TEC fluctuation during the geomagnetic storm on April 23-24, 2023 can be seen in Figures 6,7, 8, and 9. A strong geomagnetic storm occurred (initial phase) on April 23, 2023, at 23.00 UT or 06.00 local time depicted by a decrease in the Dst index reaching -109 nT. Maximum depression of the Dst index (main phase) occurred on April 24 at 06.00 UT or 13.00 local time, and the Dst index experienced a gradual recovery (recovery phase) later.

The ROTI indices at Kupang, Bandung, and Biak stations did not show any ionospheric irregularities related to scintillation on April 24 2023 although the geomagnetic storm was in the main phase whereas the Bandung station showed indications of ionospheric irregularities related to scintillation. The weak ionospheric irregularities at Manado were observed, which is indicated by the ROTI ranging from 0.2 TECU/minute to 0.5 TECU/minute ($0.20 \leq ROTI < 0.5$). Moreover, during the geomagnetic storm on 23-24, April all stations reported positive storms. Table 2 shows the ionospheric response to geomagnetic storms resulting in both positive and negative storms as well as ionospheric irregularities related to scintillation inhibitions.

Based on Table 2, the geomagnetic storm in April with a stormscale reaching below -200 nT caused all stations to respond to a positive storm compared to the March geomagnetic storm with a value still above -200 nT. The effect of the crest region of the Equatorial Ionospheric Anomaly (EIA) may have resulted in a negative storm at the Bandung station during the March storm. Additionally, the crest region of the Equatorial Ionospheric Anomaly (EIA) may have contributed to the degradation of the irregularities or an increase in scintillation during the main phase of the geomagnetic storm (Adekoya et al., 2023). Furthermore, another reason why Bandung and Manado stations still recorded ionospheric irregularities when the geomagnetic storm was in its main phase on March 24, 2023, and April 24, 2023, refers to the phase and time of the geomagnetic storm, the magnitude of the geomagnetic disturbance index (Dst), the time and location geographic observation stations (Olabode & Ariyibi, 2020).

Table 2 Ionospheric TEC and ROTI responses occurring in both positive and negative storms, as well as ionospheric irregularities related to scintillation inhibitions

Station	Geomagnetic Storm March (-163 nT)		Geomagnetic Storm April (-213 nT)	
	TEC	ROTI	TEC	ROTI
BIAK	Positive Storm	Inhibition	Positive Storm	Inhibition
MANADO	Positive Storm	Inhibition	Positive Storm	Weak
KUPANG	Negative Storm	Inhibition	Positive Storm	Inhibition
BANDUNG	Negative Storm	Moderate	Positive Storm	Inhibition

The results show that most GPS receivers used in this study record the inhibition of ionospheric irregularities due to scintillation during geomagnetic storms in March and April 2024, especially when geomagnetic storms are in the main phase. The results of this study display that on March 23, 2023, the maximum excursion of Dst occurred at 03.00 UT or 10.00 local time and at 06.00 UT or 13.00 local

time on April 24, 2023. This result emphasizes a study by (Chen et al., 2023). It was reported that the minimum Dst occurred at 10.00-14.00 local time and no ionospheric irregularities were observed at nighttime. They found that the westward electrical field during the storm should play a vital role in the inhibition of the nighttime ionospheric irregularities. The same result was also reported by (Imtiaz et al., 2023), Penetrating of Electric Field (PEF) and Equatorial Electrojet (EEJ) during the main phase between midnight and around noon is suspected to restrict the diffusion of plasma and suppress the occurrence of ionospheric plasma irregularities during the main phase.

Electron content variations in response to the geomagnetic storm on March 23-24, 2023, and April 23-24, 2023, show differences. The geomagnetic storm on March 23-24 was responded to as a positive storm, there was an increase in VTEC on March 24, 2023, at Manado and Biak stations, in contrast, it was responded to as a negative storm, and there was a decrease in VTEC on March 24, 2023, at Kupang and Bandung stations. Meanwhile, the geomagnetic storm on April 23-24 2023 was responded as a positive storm at all four GPS receiving stations. This confirms that the ionospheric response to a geomagnetic storm can be positive or negative, and varies depending on the storm event and the region of the globe (Olabode & Ariyibi, 2020; Uga et al., 2024).

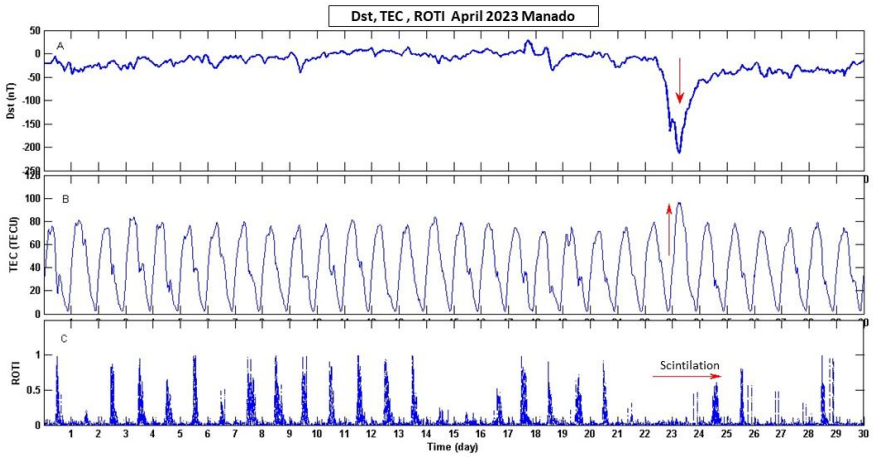

Figure 6 Dst, TEC, and ROTI indices for April at Manado

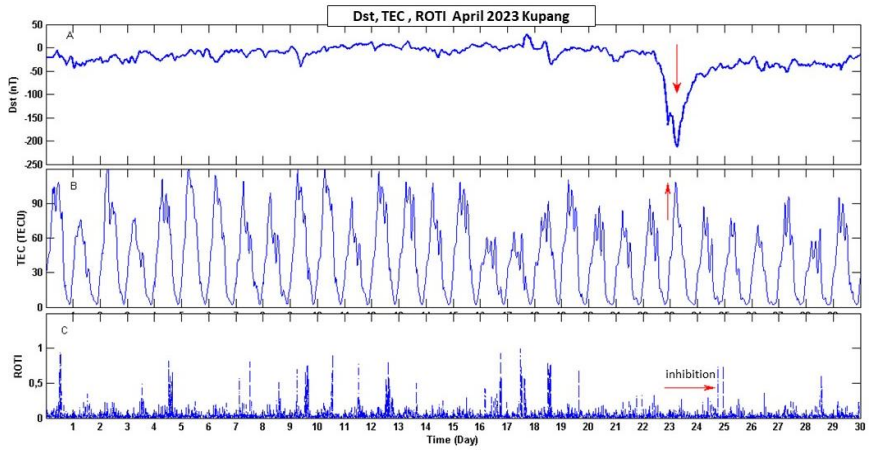

Figure 7 Dst, TEC, and ROTI indices for April at Kupang

4. CONCLUSION

Based on the ROTI index and TEC changes, the analysis of two strong geomagnetic storm events, namely on March 23-24, 2023, and April 23-24, 2023, showed suppression of plasma structure irregularities on a scale above 400 meters–several kilometers associated with scintillation and also positive/negative TEC storm responses. The emergence of scintillation (with a disturbance scale of 150

meters and above) is indeed intense in equinox months, such as March and April. An increase in ROTI per day in that month indicates the irregularities associated with ionospheric scintillation, visible from four stations. However, the geomagnetic storm coincided with the storm day that month, demonstrating the suppression of the irregularities. Similarly, the TEC response displayed both positive and negative storm activity. The TEC response at the Bandung station is particularly intriguing as irregularities continue to emerge, albeit on a smaller scale. Bandung Station, located in the crest region of ionospheric anomalies, especially the Equatorial Ionospheric Anomaly, gave the same response to positive storms. Positive and negative storm responses from TEC will impact satellite navigation signals, especially during strong geomagnetic storms. Likewise, the emergence of scintillation in the equinox month needs to be considered, especially for civil aviation using satellite-based navigation. Further case studies and additional observation stations using index scintillation (S4) or a combination of ROTI and S4 are necessary to understand these response variations better.

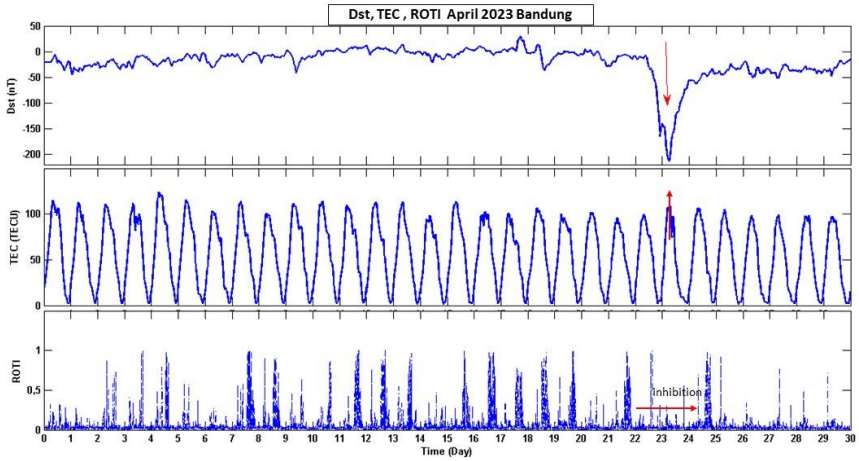

Figure 8 Dst, TEC, and ROTI indices for April at Bandung

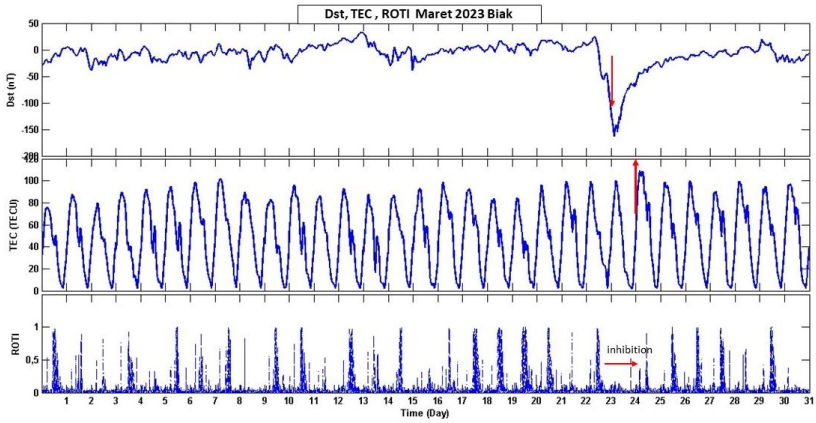

Figure 9 Dst, TEC, and ROTI indices for April at Biak

ACKNOWLEDGEMENT

This study is supported by the Ministry of Education Research and Technology of the Republic of Indonesia. Thank you to the Space Research Center, BRIN for allowing the author to access GPS receiver data for this study.

REFERENCE

Abe, O. E., Migoya-Orué, Y. O., & Radicella, S. M. (2023). Correlation analysis of normalized ROTI and S4 as

observed during different geomagnetic conditions of the 2013 September equinox over the stations within EIA African sector. *Advances in Space Research*, *72*(3), 762–774. https://doi.org/10.1016/J.ASR.2022.09.058

Adekoya, B. J., Chukwuma, V. U., Adebiyi, S. J., Adebesin, B. O., Ikubanni, S. O., Bolaji, O. S., Oladunjoye, H. T., & Bisuga, O. O. (2023). Ionospheric storm effects in the EIA region in the American and Asian-Australian sectors during geomagnetic storms of October 2016 and September 2017. *Advances in Space Research*, *72*(4), 1237–1265. https://doi.org/10.1016/j.asr.2023.04.016

Aol, S., Buchert, S., & Jurua, E. (2020). Ionospheric irregularities and scintillations: a direct comparison of in situ density observations with ground-based L-band receivers. *Earth, Planets and Space*, *72*(1). https://doi.org/10.1186/s40623-020-01294-z

Asnawi, H., Buldan, M., Joni, E., & Dyah, R. M. (2021). Test of velocity-displacement estimation using variometric method under the condition of ionospheric scintillation during equinoctial months of solar maximum period 2012. *International Journal of Physical Sciences*, *16*(1), 29–35. https://doi.org/10.5897/ijps2020.4921

Chen, D., Guo, W., Xie, Z., Xia, P., Luo, X., Ye, S., Jiang, W., & Liu, H. (2023). Ionospheric Irregularities Responses to Strong Geomagnetic Storms in Hong Kong Region Over The Past Two Solar Cycles (2001–2020). *IEEE Transactions on Geoscience and Remote Sensing*, *61*, 1–9.

Collado-Villaverde, A., Muñoz, P., & Cid, C. (2024). Classifying and bounding geomagnetic storms based on the SYM-H and ASY-H indices. *Natural Hazards*, *120*(2), 1141–1162. https://doi.org/10.1007/s11069-023-06241-1

Imtiaz, N., Dugassa, T., Calabia, A., & Kashcheyev, A. (2023). Longitudinal dependence of ionospheric irregularities to maximum ring current and PPEF sensed by GNSS and magnetometers during the storm of 4 November 2021. *Ournal of Geophysical Research: Space Physics*, *5*. https://doi.org/10.22541/essoar.168298684.44695925/v1

Kassa, Y., Tebabal, A., & Damtie, B. (2024). Nighttime ionospheric irregularity during intense geomagnetic storm events over the Europe-African longitudinal sector. *Heliyon*, *10*(19), e38138. https://doi.org/10.1016/j.heliyon.2024.e38138

Li, W., Song, S., & Jin, X. (2022). Ionospheric Scintillation Monitoring With ROTI From Geodetic Receiver: Limitations and Performance Evaluation. *Radio Science*, *57*(5), 1–15. https://doi.org/10.1029/2021RS007420

Mondal, M., Kumar, S., Banola, S., & Singh, A. K. (2024). Occurrence of ionospheric scintillations under different solar and geomagnetic conditions over low latitude station Varanasi. *Advances in Space Research*, *73*(7), 3658–3674.

Nguyen, C. T., Oluwadare, S. T., Le, N. T., Alizadeh, M., Wickert, J., & Schuh, H. (2022). Spatial and temporal distributions of ionospheric irregularities derived from regional and global roti maps. *Remote Sensing*, *14*(1). https://doi.org/10.3390/rs14010010

Nguyen Thanh, D., Le Huy, M., Amory-Mazaudier, C., Fleury, R., Saito, S., Nguyen Chien, T., Pham Thi Thu, H., Le Truong, T., & Nguyen Thi, M. (2021). Characterization of ionospheric irregularities over Vietnam and adjacent region for the 2008-2018 period. *Vietnam Journal of Earth Sciences*. https://doi.org/10.15625/2615-9783/16502

Olabode, A. O., & Ariyibi, E. A. (2020). Geomagnetic storm main phase effect on the equatorial ionosphere over Ile–Ife as measured from GPS observations. *Scientific African*, *9*, e00472. https://doi.org/10.1016/j.sciaf.2020.e00472

Ondede, G. O., Rabiu, A. B., Okoh, D., Baki, P., Olwendo, J., Shiokawa, K., & Otsuka, Y. (2022). Relationship between geomagnetic storms and occurrence of ionospheric irregularities in the west sector of Africa during the peak of the 24th solar cycle. *Frontiers in Astronomy and Space Sciences*, *9*(November), 1–17. https://doi.org/10.3389/fspas.2022.969235

Uga, C. I., Gautam, S. P., & Seba, E. B. (2024). TEC disturbances caused by CME-triggered geomagnetic storm of September 6–9, 2017. *Heliyon*, *10*(10), e30725. https://doi.org/10.1016/j.heliyon.2024.e30725

Vankadara, R. K., Panda, S. K., Amory-Mazaudier, C., Fleury, R., Devananboyina, V. R., Pant, T. K., Jamjareegulgarn, P., Haq, M. A., Okoh, D., & Seemala, G. K. (2022). Signatures of Equatorial Plasma Bubbles and Ionospheric Scintillations from Magnetometer and GNSS Observations in the Indian Longitudes during the Space Weather Events of Early September 2017. *Remote Sensing*, *14*(3). https://doi.org/10.3390/rs14030652

Zhao, X., Li, G., Xie, H., Hu, L., Sun, W., Yang, S., Li, Y., Ning, B., & Takahashi, H. (2021). The Prediction of Day-to-Day Occurrence of Low Latitude Ionospheric Strong Scintillation Using Gradient Boosting

Algorithm. *Space Weather*, *19*(12), 1–14. https://doi.org/10.1029/2021SW002884